

# UC Santa Cruz

## UC Santa Cruz Previously Published Works

### Title

CRISPRi screens identify the lncRNA, LOUP, as a multifunctional locus regulating macrophage differentiation and inflammatory signaling.

### Permalink

<https://escholarship.org/uc/item/7p5045j3>

### Journal

Proceedings of the National Academy of Sciences, 121(22)

### Authors

Halasz, Haley

Malekos, Eric

Covarrubias, Sergio

et al.

### Publication Date

2024-05-28





### DOI

10.1073/pnas.2322524121

Peer reviewed



# CRISPRi screens identify the lncRNA, *LOUP*, as a multifunctional locus regulating macrophage differentiation and inflammatory signaling

Haley Halasz<sup>a,1</sup>, Eric Malekos<sup>b,1</sup>, Sergio Covarrubias<sup>a,1</sup>, Samira Yitiz<sup>a</sup>, Christy Montano<sup>a</sup>, Lisa Sudek<sup>a</sup>, Sol Katzman<sup>a</sup> , S. John Liu<sup>c,d</sup>, Max A. Horlbeck<sup>c,d,e,f</sup> , Leila Namvar<sup>a</sup> , Jonathan S. Weissman<sup>g,h,i,j</sup>, and Susan Carpenter<sup>a,2</sup> 

Edited by Carl Nathan, Weill Medical College of Cornell University, New York, NY; received December 20, 2023; accepted April 16, 2024

Long noncoding RNAs (lncRNAs) account for the largest portion of RNA from the transcriptome, yet most of their functions remain unknown. Here, we performed two independent high-throughput CRISPRi screens to understand the role of lncRNAs in monocyte function and differentiation. The first was a reporter-based screen to identify lncRNAs that regulate TLR4-NFκB signaling in human monocytes and the second screen identified lncRNAs involved in monocyte to macrophage differentiation. We successfully identified numerous noncoding and protein-coding genes that can positively or negatively regulate inflammation and differentiation. To understand the functional roles of lncRNAs in both processes, we chose to further study the lncRNA *LOUP* [lncRNA originating from upstream regulatory element of *SPI1* (also known as *PU.1*)], as it emerged as a top hit in both screens. Not only does *LOUP* regulate its neighboring gene, the myeloid fate-determining factor *SPI1*, thereby affecting monocyte to macrophage differentiation, but knockdown of *LOUP* leads to a broad upregulation of NFκB-targeted genes at baseline and upon TLR4-NFκB activation. *LOUP* also harbors three small open reading frames capable of being translated and are responsible for *LOUP*'s ability to negatively regulate TLR4/NFκB signaling. This work emphasizes the value of high-throughput screening to rapidly identify functional lncRNAs in the innate immune system.

long noncoding RNA | macrophage | CRISPRi | short encoded peptide | inflammation

According to the latest Gencode release (version 45), the human genome encodes 20,424 long noncoding RNAs (lncRNAs) making it the largest group of genes transcribed from the genome. Due to their cell type specificity, this number continues to increase as more sequencing is performed (1). lncRNAs are transcripts over 200 nucleotides that are often spliced and polyadenylated and are without annotated or predicted protein-coding potential. Over the last decade, a number of lncRNAs have been functionally characterized and shown to play diverse roles in a variety of biological processes from cell differentiation and cancer to immunity (2–4). Yet the functions of the vast majority of these transcripts remain unknown. Historically, one of the largest challenges in studying lncRNAs has been the lack of reliable and specific approaches to target these transcripts, especially in a high-throughput manner. Because lncRNAs lack open reading frames, these genes are not susceptible to frameshift mutations induced by classic CRISPR/Cas9. Recently the adoption of the modified CRISPR/Cas9 technology, CRISPR inhibition (CRISPRi), has become a powerful tool for interfering with transcription of lncRNAs by inducing repressive chromatin marks at the transcription start site, making it an attractive approach to discover functional lncRNAs. Advanced computational developments in single guide RNA (sgRNA) library design coupled with targeted transcriptional repression induced by the components of CRISPRi have made it possible to rapidly identify many functional lncRNA loci in a single pooled screening experiment (5).

A small number of high-throughput screens have been performed to identify functional lncRNAs (5–8) but very few have been performed in immune cells (9). To obtain insights into innate immunity, more specifically monocyte and macrophage biology, we conducted two pooled CRISPRi screens in human monocytic cells (THP1s). In one screen, we sought to identify lncRNAs that regulate monocyte to macrophage differentiation, while the second assessed for lncRNAs that modulate NFκB signaling. Monocyte to macrophage differentiation is a highly coordinated process crucial to a well-regulated inflammatory response (10, 11). Acute activation of NFκB signaling in monocytes is imperative for proper recognition and resolution of pathogens. Therefore, it is important that we gain a more complete molecular understanding of both monocyte differentiation and NFκB regulation, as dysregulation of either of these processes can lead to a diseased state (12, 13). In order

## Significance

Macrophages are critical to a well-functioning immune response, and here, we employed CRISPRi-based pooled screening to rapidly identify long noncoding RNAs (lncRNAs) functioning in macrophage differentiation and the inflammatory response. We identified 73 regulators and focused on the mechanisms of a top hit from both screens, *LOUP* [lncRNA originating from upstream regulatory element of *SPI1* (also known as *PU.1*)]. We showed that *LOUP* regulates *SPI1* in cis in a highly conserved manner. We have identified small open reading frames-encoded peptides that are produced from the *LOUP* locus that negatively regulate the TLR4-NFκB signaling cascade in addition to regulating *SPI1* posttranscriptionally. Overall, our work highlights the power of high-throughput CRISPRi screens and brings to light the intriguing bimodal function of *LOUP*.

Competing interest statement: S. Carpenter is a paid consultant for NextRNA Therapeutics.

This article is a PNAS Direct Submission.

Copyright © 2024 the Author(s). Published by PNAS. This open access article is distributed under Creative Commons Attribution-NonCommercial-NoDerivatives License 4.0 (CC BY-NC-ND).

<sup>1</sup>H.H., E.M., and S. Covarrubias contributed equally to this work.

<sup>2</sup>To whom correspondence may be addressed. Email: [sucarpen@ucsc.edu](mailto:sucarpen@ucsc.edu).

This article contains supporting information online at <https://www.pnas.org/lookup/suppl/doi:10.1073/pnas.2322524121/-/DCSupplemental>.

Published May 23, 2024.

to conduct the two screens, we developed a sgRNA library targeting over 2,000 THP1-expressed lncRNAs. Utilizing our NFkB (RelA/p65) reporter THP1 CRISPRi line, we identified 35 regulators of NFkB. We utilized phorbol esters (PMA) to initiate differentiation and identified 38 lncRNAs regulating monocyte to macrophage differentiation. We were intrigued to find that one lncRNA, *LOUP*, was a top hit in both screens. Interestingly, *LOUP* neighbors the gene *SPI1*, a myeloid fate-determining transcription factor required for development of monocytes and macrophages. Since many functional lncRNAs exhibit *cis*-regulatory effects, including *LOUP* (14), we sought to further investigate *LOUP*'s role as a *cis* regulator of *SPI1*. While Trinh et al., previously demonstrated that *LOUP* RNA mediates direct interactions with the *SPI1* promoter and the transcription factor RUNX1 in unstimulated monocytes, we found that *LOUP* and *SPI1* occupy a topologically associating domain (TAD) that is maintained in THP1s before and after differentiation and found evidence of a prominent super enhancer (SE) in this TAD (15). The TAD and superenhancer are conserved in mouse bone marrow-derived macrophages (BMDMs) and dendritic cells (BMDCs), highlighting the cross-species importance of *cis*-regulatory activity and chromatin structure at this locus in monocytes and their derivative cell types.

While we were able to verify that *LOUP* exhibits a *cis*-regulatory effect on *SPI1*, this did not account for its role as a negative regulator of NFkB. More recent discoveries in the field of lncRNA biology have uncovered bifunctional lncRNAs, where the RNA transcript can carry out *cis* or *trans*-effects, but can also produce functional short, encoded peptides (SEPs) from short open reading frames (sORFs) (16). We analyzed ribosome sequencing (Ribo-Seq) and conservation data and found that *LOUP* is translated and harbors sORFs that are well conserved in monkeys and apes. We conducted functional experiments that demonstrate that *LOUP* SEPs can function to negatively regulate inflammation in addition to regulating *SPI1* posttranscriptionally in human THP1 cells. Together, this work defines an unappreciated role for the *LOUP* locus in regulating critical immune processes, which was enabled by unbiased high-throughput CRISPRi screening.

## Results

**CRISPRi Screen Identifies lncRNAs that Regulate NFkB and Macrophage Differentiation.** To begin to define lncRNAs that regulate NFkB signaling in human macrophages, THP1 cells containing five NFkB (p65) binding sites upstream of a minimal CMV-driven EGFP, as well as deactivated Cas9-KRAB (dCas9-KRAB), were transduced with pooled lentivirus (MOI = 0.3) generated from our custom sgRNA library containing ~25,000 individual sgRNAs (Dataset S1). The sgRNA library was designed using the hCRISPRi-v2.1 algorithm (5), with 10 sgRNAs targeting the transcription start sites of 2,342 lncRNAs annotated in the human genome assembly GRCh37 (hg19). lncRNA sgRNA target sites were determined based on expression in RNA-seq data from THP1s generated by our lab and previously published p65 ChIP-seq data and Fantom transcription start site (TSS) information (17) (Fig. 1A). The same design and cloning strategy were used as previously described (5).

For the NFkB reporter screen, cells were stimulated with LPS for 24 h and then sorted by flow cytometry-assisted cell sorting (FACS). For each replicate, the top and bottom 20% of GFP+ gated cells were collected, and genomic DNA was isolated from the GFP<sup>hi</sup>, GFP<sup>lo</sup>, and unsorted populations. This gating strategy was determined based on earlier reporter-based sorting screens to sufficiently capture nontargeting controls (17–20). In each resulting population, sgRNAs were PCR amplified and then sequenced (Fig. 1A).

MAUDE (21) analysis was performed comparing each GFP<sup>hi</sup> and GFP<sup>lo</sup> population to the unsorted (Fig. 1B). Genes with combined Z-scores (Stouffer's method) of less than -3 were defined as significant positive regulators of NFkB, while genes with combined Z-scores above 3 were defined as significant negative regulators (SI Appendix, Fig. S1 and Datasets S2 and S3) (Fig. 1B and C).

To screen for regulators of monocyte to macrophage differentiation: following selection, cells were treated three times over the course of 11 d with 2 nM PMA allowing for 50% of cells to differentiate (adhere to the plate), ensuring identification of both positive and negative regulators of differentiation (Fig. 1A). Thirty-eight lncRNAs were identified with a Mann-Whitney U-score greater than 3 or less than -3 (67 had a *p*-value cut-off of <0.01) (SI Appendix, Fig. S2 and Datasets S4–S6) as regulators of differentiation with over 75% representing positive regulators of the pathway (Fig. 1D and E).

Given that our sgRNA library included lncRNA genes regardless of genomic location, many of the targets are very near to or overlapping with neighboring genes. Heterochromatin induced by the dCas9-KRAB has been shown to reach as far as 1 kb so we considered this caveat when choosing a top candidate lncRNA to further functionally validate (5, 21). Ten of the top 35 NFkB hits and 8 of the top 38 PMA hits are intergenic, defined as having their own promoters at least 1 kb away from promoters of neighboring protein-coding genes (SI Appendix, Figs. S1 and S2). Five top NFkB hits, *LRF1*, *UHRF1*, *SMIM27*, *CASP8AP2*, and *KMT2B*, were previously annotated as noncoding transcripts by Gencode, but have now been annotated as coding genes (SI Appendix, Fig. S1). One additional hit, *MIR155HG* has a documented dual function as a host gene of micro-RNA 155 and as encoding a 17 amino acid peptide from its sORF (22). Two PMA hits were also found to now be annotated as protein-coding, *TEN1* and *ZNF506*. The other top hits are annotated either from a bidirectional promoter or antisense and overlapping to coding genes. In these cases, it is possible that the dCas9-KRAB has disrupted transcription of both bidirectional and overlapping transcripts. Interestingly, none of the coding genes targeted have been previously identified as regulators of NFkB or monocyte differentiation and represent coding regulators of the pathway and therefore are still of interest (SI Appendix, Figs. S1 and S2). Surprisingly, seven lncRNAs and one protein-coding gene (*ENSG00000267811*, *Nepro-AS1*, *SNHG9*, *ENSG00000261659*, *ENSG00000272434*, *ENSG00000264772*, *LOUP*, and *SMIM27*) were hits in both screens (SI Appendix, Figs. S1 and S2), suggesting genes playing multiple functions in monocyte/macrophage biology but only *LOUP* is intergenic and neighbors a gene known to regulate myeloid differentiation (*SPI1*). Of the top 10 intergenic lncRNA hits from the NFkB screen, *LOUP* is one of two genes with a coding neighbor (*SPI1*) that has been previously implicated in inflammation. The other, *LINC02528*, resides 60 kb from the promoter of *TNFRIP3* (A20), a known negative regulator of NFkB. Of the top eight intergenic lncRNA hits from the differentiation screen, *LOUP* is the only lncRNA that neighbors a coding gene known to regulate differentiation. Three other top intergenic lncRNAs hits, *SNHG12*, *LINC01220*, and *ENSG000001220*, neighbor coding genes that are involved in transcription regulation.

### ***LOUP* Shares a Conserved Topologically Associating Domain with *SPI1* and Is Highly Expressed in Human and Mouse Monocytes.**

Given that *LOUP* (lncRNA originating from the upstream regulatory element of *SPI1*) arose as a top hit in both screens and is intergenic, we wished to determine mechanistically how it can be involved with two different biological processes in monocytes. Given the recent evidence that *LOUP* acts as an enhancer for its neighboring gene *SPI1* (14), and the evidence of a conserved

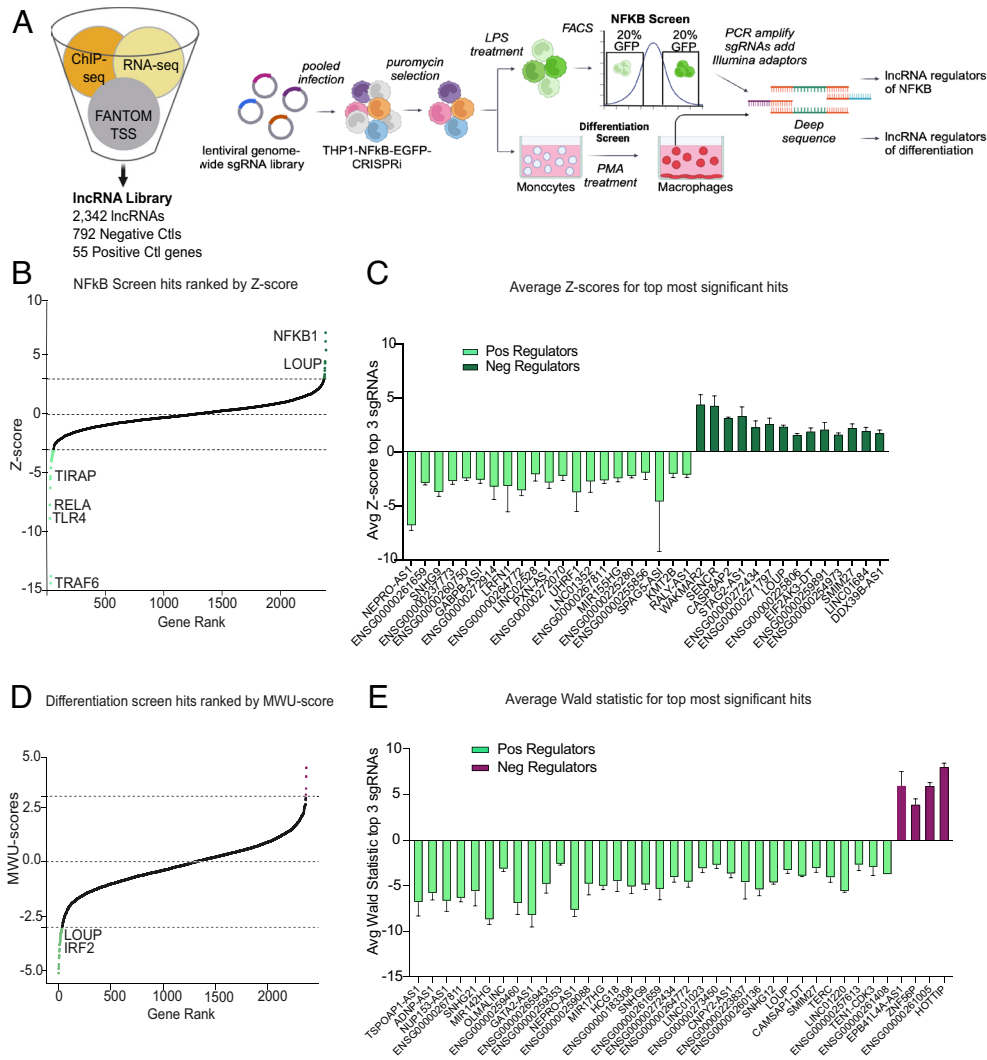


**Fig. 1.** CRISPRi screens identify positive and negative regulators of NfκB and macrophage differentiation. (A) Overview of sgRNA library design and overview of the screen. sgRNAs were designed to target the transcription start sites of over 2,000 Gencode hg19 annotated lncRNAs. Transcription start sites were predicted using data from FANTOM and ENCODE. THP1 lncRNA expression was estimated from THP1 RNA-seq data. NfκB-EGFP-CRISPRi-THP1 cells were infected with pooled sgRNA libraries, selected, stimulated with LPS, and then sorted based on the top and bottom 20% of EGFP fluorescence. sgRNAs from the resulting GFP-expressing populations were PCR amplified and sequenced. The same untreated THP1s containing the sgRNA library were treated with PMA and undifferentiated cells were collected 11 d posttreatment. sgRNAs from each timepoint were PCR amplified and sequenced. (B) NfκB screen analysis. Analysis was performed on each of three screen replicates comparing sgRNA enrichment in the GFP low population or the GFP high population to the unsorted population with the MAUDE tool. Z-scores across replicates were combined by Stouffer's method and ranked in order of Z-score. Z-score cutoffs of  $-3$  and  $3$  are considered significant as highlighted in light green (positive regulators) and dark green (negative regulators). Genes labeled are significant known protein-coding regulators of NfκB that acted as positive controls in the screen. (C) Significant NfκB hits. The average z-scores of the top three best-scoring sgRNAs for all significant hits with SD. (D) PMA screen analysis. DESeq2 was used to establish log2foldchange (L2FC) of sgRNAs between no treatment and PMA conditions. L2FC for sets of sgRNAs targeting each gene were compared to L2FC of all negative controls by the Mann-Whitney U (MWU) test. MWU scores of  $-3$  and  $3$  are considered significant. (E) Significant differentiation hits. The average Wald test statistic of the top three best-scoring sgRNAs for all significant hits with SD.

*SPI1* SE spanning the locus in humans and mice (15), we examined H3K27Ac ChIP-Seq in THP1s (23). ATAC-seq showed open chromatin at *LOUP* and ChIP-Seq analysis found broad deposition of H3K27Ac marks indicating that the *LOUP* locus meets the more expansive SE criteria (24) (Fig. 2A). Given the evidence of an important SE, we hypothesized that local chromatin structure would have important regulatory functions and called TADs from Hi-C data (23). CTCF ChIP-seq and chromosome interactions frequencies indicate that *LOUP* and *SPI1* occupy the same TAD (Fig. 2A). GTEx gene expression shows that *LOUP* and *SPI1* are expressed almost exclusively in blood cells in contrast to neighboring genes outside the TAD, demonstrating that they are members of a distinct domain (SI Appendix, Fig. S3).

Since *LOUP* was a hit in the PMA differentiation screen, we performed epigenetic analysis on data from PMA differentiated

THP1s. We found the Hi-C, ChIP-seq, and ATAC-seq patterns to be consistent after PMA treatment, indicating that local epigenetic changes are not primarily responsible for differences in *SPI1* or *LOUP* expression following differentiation. Epigenetic marks are also consistent in mouse BMDMs and BMDCs compared to human macrophages indicating that the epigenetic landscape is strongly conserved in differentiated monocyte-derived cells across species (Fig. 2B). Despite this remarkable level of conservation, we find evidence that the *LOUP* transcript itself has diverged between humans and mice. Whereas human *LOUP* is a distinct gene, in mice, we find that the equivalent locus is transcribed as either a two-exon lncRNA (*Loup*) or as an extended 5'-UTR of *Spi1* (Fig. 2C). While there is evidence from the Havana database of a possible extended 5' UTR in human *SPI1* (ENST00000713543) we do not see any evidence of such a transcript in our human



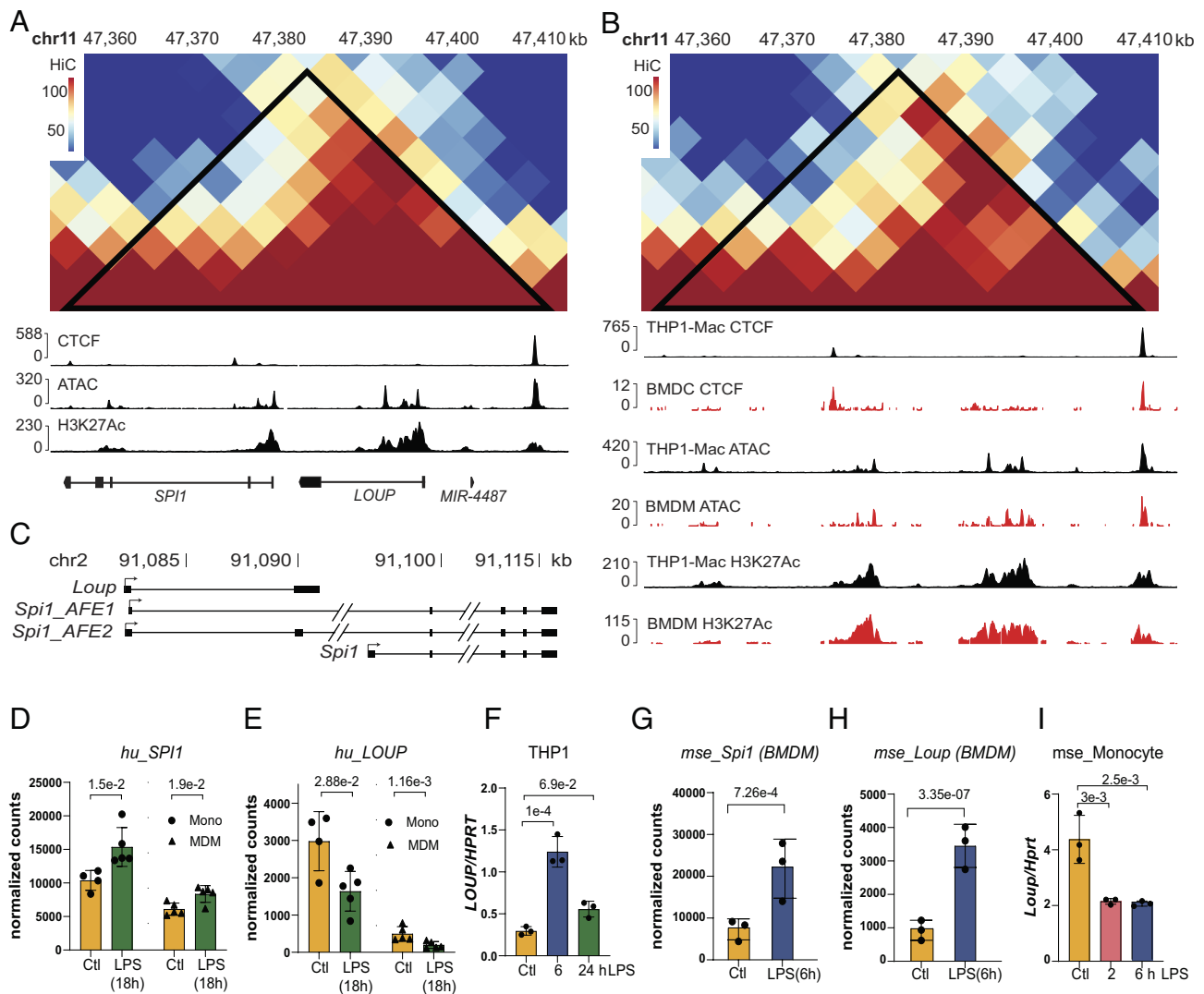


**Fig. 2.** *LOUP* shares a TAD with *SPI1* and is highly conserved in monocytes. (A) Predicted TAD for *LOUP* and *SPI1* in THP1s. Browser tracks display regions of CTCF binding, ATAC peaks, and regions of high H3K27 acetylation. Numbers on the y axis represent raw read counts. (B) Conserved TAD and epigenetic marks following differentiation in humans and mice. PMA differentiated THP1-macrophages (THP1-Macs) maintain chromatin structure and epigenetic marks at the *LOUP/SPI1* locus. Patterns of epigenetic marks and CTCF binding are also conserved in mouse BMDMs and BMDCs. (C) *Loup* and *Spi1* isoforms in mouse. Gene models of transcripts at *Spi1* locus determined from long-read Nanopore on BMDMs and called with FLAIR. (D–J) Effect of LPS Stimulus on *LOUP* and *SPI1* Expression in human and mouse cells. (D and E) *SPI1* (D) and *LOUP* (E) expression in human monocytes and monocyte derived macrophages. Differential gene expression was calculated from RNA-Seq of untreated or LPS treated monocytes and macrophages. Significance represented by the adjusted *p*-value of DESeq2 implementation of the Wald test. (F) qPCR of *LOUP* in THP1 qPCR measurement of *LOUP* across three replicates of human THP1 cells untreated or treated with LPS for 6 or 24 h. *LOUP* expression increases at 6 h of LPS treatment and comes back down to a nonsignificant change compared to baseline by 24 h. Values are normalized to HPRT. Error bars show SD and significance testing was performed with one-way ANOVA with Dunnett's multiple comparisons in GraphPad Prism. (G and H) *Spi1* (G) and *Loup* (H) expression in mouse bone marrow-derived macrophages. Differential gene expression was calculated from RNA-Seq of untreated or LPS treated BMDMs. Significance represented by the adjusted *p*-value of DESeq2 implementation of the Wald test. (I) qPCR of *Loup* in mouse monocytes qPCR measurement of *Loup* across three replicates of primary mouse monocytes untreated or treated with LPS for 2 or 6 h. *Loup* expression decreases in both LPS-treated conditions relative to untreated control. Values are normalized to *Hprt*. Error bars show SD and significance testing was performed with one-way ANOVA with Dunnett's multiple comparisons in GraphPad Prism.

long-read data (25). Moreover, the *LOUP/Loup* sequences are only 37% identical and have dissimilar predicted secondary structures (SI Appendix, Fig. S4).

We next examined the expression levels of *LOUP* and *SPI1* across human and mouse monocytes and macrophages at baseline and following LPS stimulation. Interestingly, *SPI1* and *LOUP* are dominantly expressed in primary monocytes compared to differentiated macrophages (Fig. 2 D and E). *SPI1* is consistently induced following LPS (Fig. 2 D and G), while *LOUP* appears to be reduced in expression in primary human and mouse monocytes following LPS (Fig. 2 E and J) but induced in human monocyte cell line THP1 and mouse macrophages (Fig. 2 F and H). These differences in expression patterns of *LOUP/Loup* might be explained by the complexity of the locus and the possible isoforms

being produced as outlined in Fig. 2 C and SI Appendix, Fig. S5. Together, these data indicate a high level of epigenetic conservation at the *LOUP* and *SPI1* loci suggestive of the importance for *LOUP* as a *cis* regulatory enhancer during the process of myeloid differentiation as recently described (14). Differences in expression of *LOUP* and *SPI1* following induction of inflammation with LPS and differences observed between human and mouse monocytes and macrophages indicate potentially differing roles for these genes post myeloid cell fate.

***LOUP* Acts to Negatively Regulate NFκB Target Genes at the RNA and Protein Level.** Based on the results of the screen, *LOUP* can negatively regulate NFκB activation (Fig. 1 B and C). We aimed to look broadly at inflammatory gene expression upon *LOUP* knockdown

(LOUP-KD). To this end, we generated three independent sgRNA lines targeting *LOUP* and confirmed knockdown by qPCR compared to a scrambled control line (Fig. 3A). RNA was collected from two

of the *LOUP*-KD lines (sgRNA\_1 and sgRNA\_2) both before and after 6 h of LPS stimulation. Using Nanostring technology (Immune gene panel) to directly quantify RNA transcripts of over 500

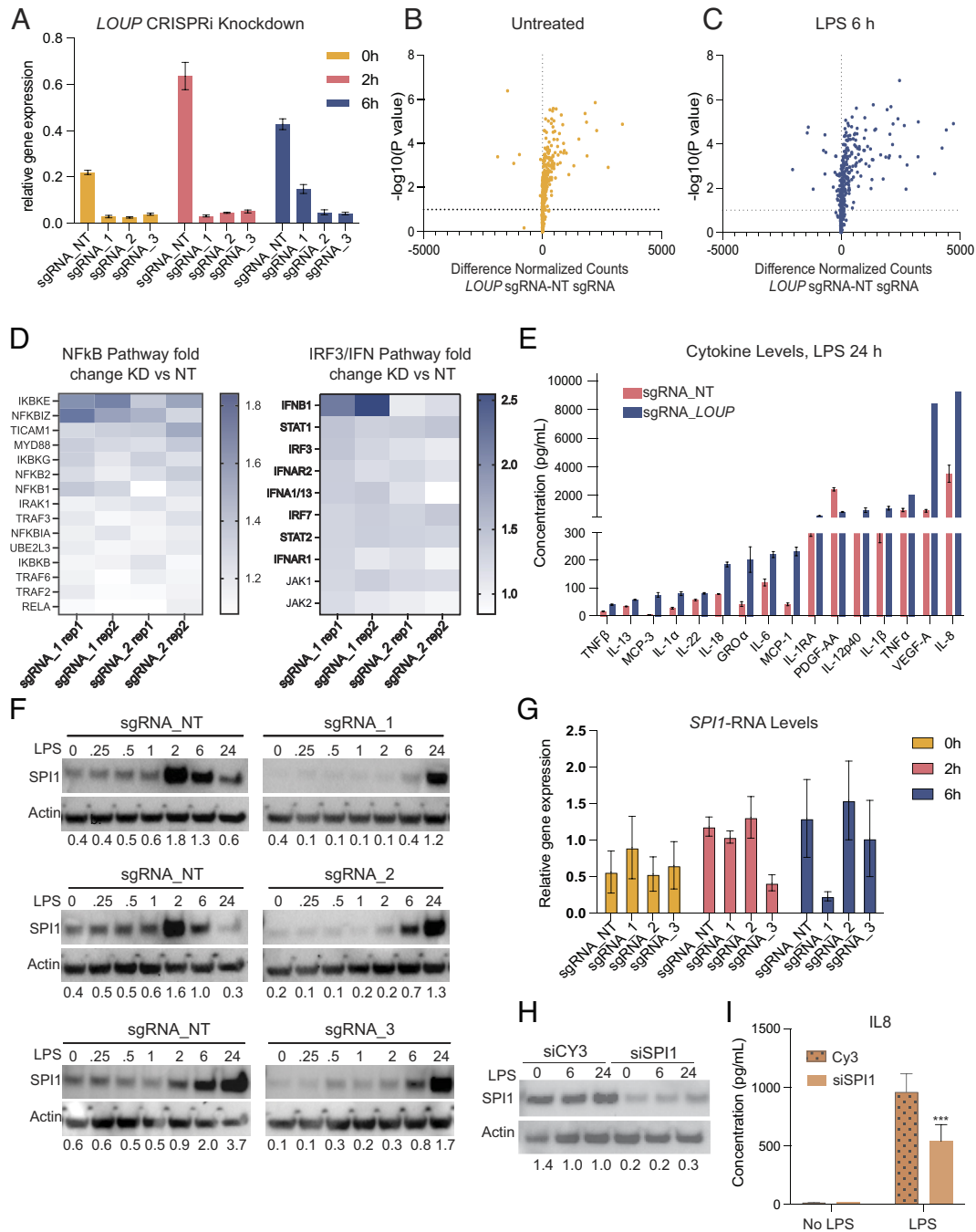


**Fig. 3.** Knockdown of *LOUP* upregulates NfκB targeted genes. (A) CRISPRi Knockdown of *LOUP* in THP1s. Three additional sgRNAs (sgRNAs 1, 2, 3) were designed to target top lncRNA candidate *LOUP*. qPCR measurement of *LOUP* across three replicate experiments shows knockdown of *LOUP* by all three sgRNAs ( $p$ -values  $< 0.05$ ) vs. a nontargeting control sgRNA (NT) before LPS stimulation (0 h) and after 2 and 6 h of LPS stimulation. Values are normalized to *HPRT* and error bars represent SD. (B and C). Multiplexed analysis of immune-related transcripts upon *LOUP* knockdown. (B and C) Transcripts of 580 immune genes were measured in RNA from a nontargeting control and 2 of the sgRNA *LOUP* knockdowns at baseline and after 6 h of LPS stimulation. Each sample was measured in duplicate. All transcript counts were normalized to six housekeeping genes then both knockdowns and duplicate measurements were averaged. All genes were plotted regardless of the  $p$ -value. (D) Heat map representing fold change of knockdowns vs. nontargeting control at baseline for NfκB pathway genes (Left panel) and IFN pathway genes (Right panel) significantly upregulated in transcript analysis (B) ( $p$ -values  $< 0.05$ ). (E) Multiplexed ELISA of cytokines upon *LOUP* knockdown. ELISA was performed on the supernatant from three nontargeting controls and all three *LOUP* knockdowns after 24 h LPS treatment. All bars represent an average of all three nontargeting (NT) or an average of all three knockdowns with SD. All differences observed between NT and knockdowns for each cytokine are significant ( $p$ -values  $< 0.05$ ). (F) Western blot analysis of SPI1. Nontargeting control (NT) vs. 3 *LOUP* knockdowns (sgRNAs 1, 2, 3) over a time course (hours) of LPS treatment. Samples were collected at baseline (0), 15 min (0.25), 30 min (0.5), 1 h (1), 2 h (2), 6 h (6), and 24 h (24). Quantitative values indicate densitometry ratios of SPI1:Actin. (G) SPI1 mRNA levels following *LOUP* knockdown. *SPI1* was measured by qPCR in the three THP1 CRISPRi *LOUP* knockdown cells. (H) Knockdown of SPI1. Western blot analysis of SPI1 in WT THP1 cells transfected with a *SPI1* targeting siRNA (siSPI1) compared to a control nontargeting siRNA (siCy3). Samples were collected at baseline (0) and after 6 and 24 h of LPS treatment. Quantitative values indicate densitometry ratios of SPI1:Actin. Blot is representative of three separate experiments. (I) Effect of SPI1 knockdown on IL8. IL8 ELISA was performed on supernatant from control and *SPI1* siRNA THP1s treated with LPS for 24 h. Bars represent an average of two separate experiments each measured in triplicate with SD ( $p$ -value  $< 0.0005$ ).

immune genes, most of which are NFkB targets, it was evident that knockdown of *LOUP* results in broad upregulation of transcription of inflammatory genes both before and after LPS stimulation (Fig. 3 *B* and *C*), including transcripts that comprise both the TLR4/NFkB and IRF3/IFN signaling pathways (Fig. 3*D*). To determine whether knockdown of *LOUP* affected protein levels of inflammatory genes, we collected supernatant 24 h post LPS treatment from all three *LOUP* knockdown THP1 cell lines and performed cytokine arrays testing 45 proteins. Of note, 16 of the 45 inflammatory cytokines were significantly increased compared to controls, with IL8 being the most upregulated (Fig. 3*E*).

Given the evidence that *LOUP* may act as an enhancer for its neighboring gene *SPI1* (Fig. 2 *A* and *B*) (14), and that this is true for other lncRNAs neighboring critical protein regulators such as the lncRNA *lincRNA-Cox2* and *PTGS2* (26), and *lincRNA-p21* and its protein-coding neighbor p21 (27) we wanted to determine whether a reduction in *SPI1* could be responsible for the negative regulation of NFkB or inflammatory signaling. First, we stimulated cells with 200 ng/mL LPS for the outlined time course and measured SPI1 levels by western blot (Fig. 3*F*). In THP1 cells, SPI1 is present at baseline and is strongly induced between 2 and 6 h following LPS stimulation in nontargeting control cells (Fig. 3*F*). Perhaps most interesting is the comparison of SPI1 levels between each of the control replicates and three different *LOUP* knockdowns at baseline where SPI1 is down-regulated when *LOUP* is knocked down. In the *LOUP* knockdown lines, SPI1's induction peaks after 24 h of LPS to the levels observed in the control lines after 2 to 6 h, indicating that *LOUP* increases SPI1 levels early in inflammation (Fig. 3*F*). Given the evidence that *LOUP* functions as an enhancer, we were surprised to find that our CRISPRi *LOUP* targeting sgRNAs (Fig. 3*A*) did not reduce *SPI1* RNA expression (Fig. 3*G*).

To separate out the possible role for SPI1 as a negative regulator of NFkB with that of *LOUP*, we transfected wild-type THP1s with siRNA targeting *SPI1* or a nontargeting siRNA control (siCY3) and knockdown was confirmed by western blot (Fig. 3*H*). IL8 was measured in the *SPI1* knockdown vs. control by ELISA as this was one of the most impacted cytokines in response to *LOUP* knockdown. In contrast to *LOUP* knockdown, *SPI1* knockdown resulted in significantly decreased levels of IL8 (Fig. 3*I*). This is consistent with the role of *SPI1* as a positive regulator of inflammation and suggests that loss of *SPI1* alone may not be responsible for the broad increase in inflammatory gene transcription (28–30). *SPI1* has exhibited important roles as both a transcriptional repressor and activator that are very context and timing specific (31–33). To investigate this in our system, we knocked down *SPI1* using siRNA in our NFkB-THP1 reporter line and did not observe any major impact on the reporter utilized in the screen (*SI Appendix*, Fig. S6). This indicates that there is a distinct role for *LOUP* as a negative regulator of NFkB, independent of *SPI1*'s role as a transcriptional regulator of inflammatory genes.

***LOUP* sORF Encoded Peptides (SEPs) Function to Regulate NFkB Genes and SPI1 Protein.** To determine *LOUP*'s mechanism of action in regulating inflammatory genes, we first determined its localization in macrophages following fractionation and qPCR. *LOUP* RNA was detected in both the nucleus and the cytoplasm (Fig. 4*A*). Nuclear localization is consistent with its roles in *cis* regulation within the shared TAD with *SPI1*, and we reasoned that its dominant expression in the cytoplasm could explain the effects seen more broadly on gene targets of NFkB. It has been found that some cytoplasmic lncRNAs harbor short open reading frames capable of producing peptides less than 100 amino acids in length, and that these peptides can carry out important functions (34).

To investigate the coding potential of *LOUP*, we first examined existing Ribo-Seq datasets from THP1s and primary macrophages (Fig. 4*B*). Based on ribosome footprints, we established that *LOUP* harbors three sORFs with potential for translation.

Of the two *LOUP* transcript models established from our published isoform-level transcriptome atlas of macrophages (27), only the longer transcript, *LOUP*-Tx1, contains all three ORFs, while the shorter transcript, *LOUP*-Tx2, is limited to ORF3 (Fig. 4*B* and *C*). We note that despite ORF1 initiating at the 5'-most ATG, the putative 5'UTR in this case is only 14 nucleotides and recent evidence suggests that such short UTRs can favor translation initiation from downstream start codons (35). Taken together, the evidence of translation from all three ORFs is consistent with different TSS usage and low initiation stringency from a short 5'UTR.

To determine whether disruption of any sORFs resulted in an increase of inflammatory cytokines at baseline in accordance with the CRISPRi results, we targeted the sORF regions in THP1s with active CRISPR/Cas9 (Fig. 4*C*). We measured transcript levels of *IKBKE* and *NFKBIZ* (Fig. 4*D* and *E*) as transcripts from these two genes were most significantly upregulated at baseline in the *LOUP* CRISPRi knockouts (Fig. 3*D*). Interestingly both genes were significantly upregulated by the sgRNA targeting ORF1 and ORF2, but not the sgRNAs uniquely targeting ORF2 or targeting ORF2 and ORF3 (Fig. 4*D* and *E*). RNA expression levels of *LOUP* and *SPI1* were unaffected by the active CRISPR/Cas9 targeting of the ORFs (Fig. 4*F* and *G*).

To determine whether it is possible that the potential ORFs within *LOUP* might impact *SPI1* expression directly we revived our stocks of CRISPRi-mediated knockdown lines and performed RNA-Seq on them as monocytes and following differentiation for 24 h with PMA into macrophages. We observed a consistent phenotype of increased inflammatory gene expression at baseline when *LOUP* was removed from monocytes (Fig. 4*H*) similar to the nano-string data. (Fig. 3 *B* and *C* and *Dataset S10*). Interestingly, these cells do not have any impact on *SPI1* RNA either as monocytes or as differentiated macrophages (Fig. 4 *H* and *I*). To determine whether *LOUP* can posttranscriptionally regulate *SPI1* expression we first tested the translational potential of these three sORFs, with each cloned in-frame with GFP to create a translational fusion and introduced into THP1-NFkB-CRISPRi cells. Measurable GFP expression was driven by all three sORFs (Fig. 4*J*). Structural predictions of the three ORF peptides were determined using AlphaFold, but were mostly of low confidence except for an N-terminal alpha helix in the ORF2 peptide (36) (*SI Appendix*, Fig. S7). Then, to determine whether the ORFs could impact *SPI1* protein levels, we took the *LOUP* CRISPRi knockdown cells which show decreased *SPI1* compared to negative control cells (NT Ctl, Fig. 4*K*) and reconstituted them with each sORF-GFP or with the *LOUP*-RNA without start codons. All ORFs resulted in increased *SPI1* protein levels but the *LOUP* RNA alone did not (Fig. 4*K*). None of the reconstituted lines had increased *SPI1* RNA consistent with *LOUP* SEPs mediating a posttranscriptional effect on the protein (Fig. 4*L*).

We next looked at conservation of the sORFs and found that ORF1 and ORF2 are highly conserved in primates (Fig. 4 *M* and *N*) while ORF3 is not. There is no evidence of conservation of the ORFs in mice (*SI Appendix*, Fig. S8*A*). Furthermore, when we knocked down *Loup* using CRISPRi in murine BMDMs, we did not observe any impact on *Spi1* either at the protein or RNA levels indicating that the posttranscriptional effects (*SI Appendix*, Fig. S8 *B–F*) of *LOUP* on *SPI1* are likely specific to primates. Together, these data provide evidence that *LOUP* is a bimodal locus capable of regulating its neighboring gene through an enhancer mechanism during myeloid differentiation as well as encoding an SEP that functions to regulate

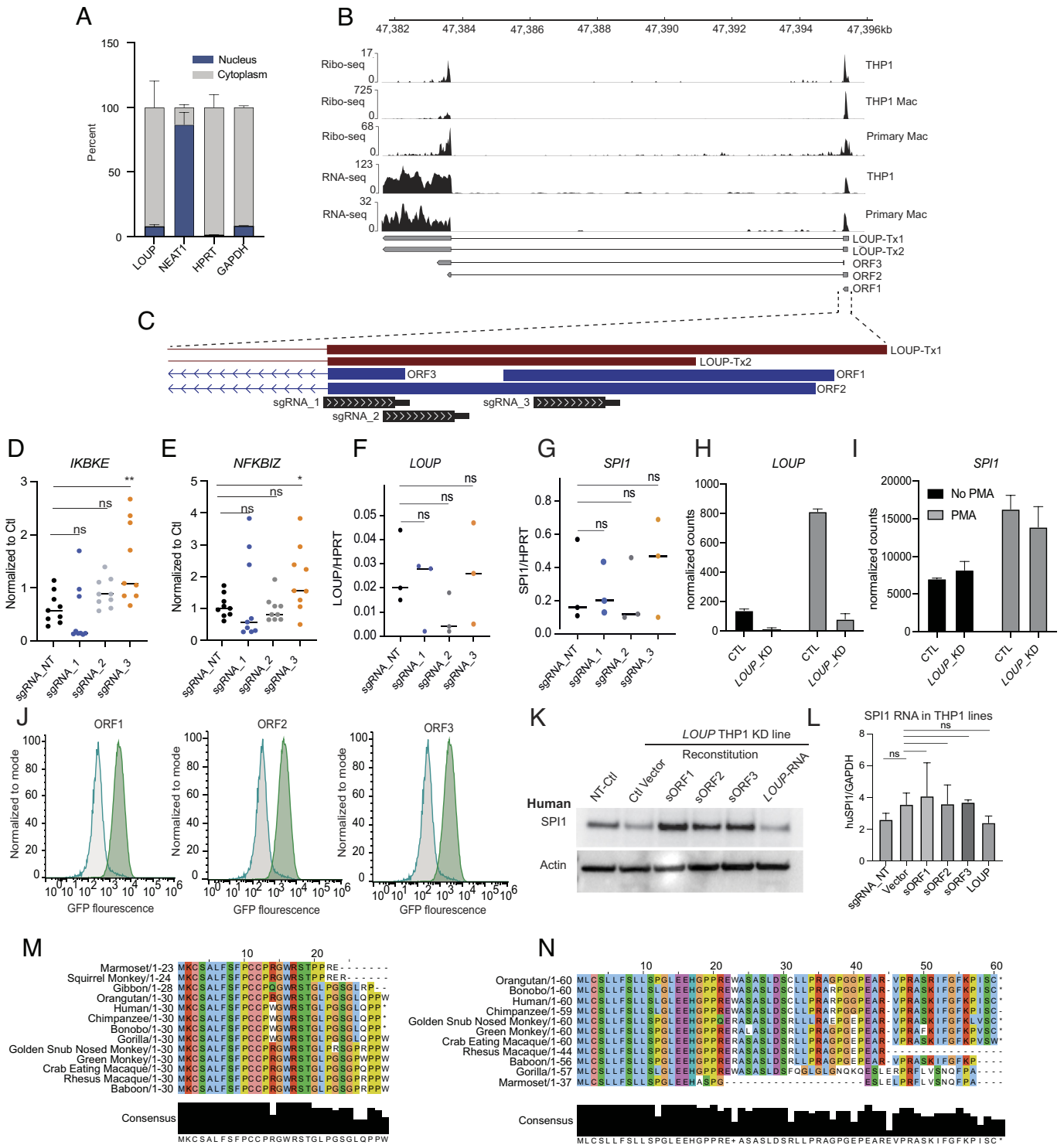


**Fig. 4.** *LOUP* encodes SEPs that regulate SPI1 protein levels and NfκB target genes. (A) Cellular localization of *LOUP* in THP1s. Nuclear/cytoplasmic fractionation of WT THP1 cells after 6 h of LPS stimulation. Data are from a single experiment with propagated error calculated for triplicate measurements. (B) *LOUP* sORF translation. Annotations of two *LOUP* isoforms and of three sORFs predicted for *LOUP* gleaned from Ribo-Seq tracks generated from THP1s, differentiated THP1s and primary macrophages. Also included are tracks for short-read RNA-seq from THP1s and long-read RNA-seq (R2C2) from primary macrophages. (C) Cas9 targeting of sORFs. *LOUP* isoforms showing the use of two transcription start sites and the translation initiation positions of sORFs, followed by depiction of sgRNAs targeting sORFs with CRISPR/Cas9. sgRNAs 1-3 correspond to panels D-G. (D-G) sORF regulation of inflammatory genes. Two of the most upregulated genes in the *LOUP* CRISPRi knockdowns were measured in *LOUP* Cas9 sORF targeted cells. Expression of *IKBKE* and *NFKBIZ* were measured at baseline in addition to *LOUP* and *SPI1* by qPCR in each of 3 Cas9 cell lines (sgRNA\_1, sgRNA\_2, sgRNA\_3) along with a nontargeting control (sgRNA\_NT) (ns = not significant, \**p*-value < 0.05, \*\**p*-value < 0.01). (H and I) *LOUP* regulation of *SPI1* transcription. RNA-Seq normalized expression levels of *LOUP* (H) and *SPI1* (I) in THP1 CRISPRi control (Ctl) or *LOUP* knockdown cells in monocytes (no PMA) or following differentiation with PMA. J. Expression of *LOUP* ORF-GFP. Flow cytometry measuring GFP expression in *LOUP* knockdown THP1s transfected with sORF-GFP fusion constructs. (K and L) Reconstitution of *LOUP* knockdown cells with *LOUP* sORFs. *LOUP* CRISPRi knockdown THP1 cells were reconstituted with sORF-GFP constructs from J and expression levels of SPI1 were measured at the protein level by western blot (K) and RNA levels by qPCR (L). (M and N) Conservation of sORFs. Human sORF sequences were aligned to genome assemblies of other primates with Blat, then sequences were translated.



SPI1 at the protein levels and broadly regulate NFkB target genes in monocytes.

## Discussion

Here, we have described genome-wide pooled CRISPRi screening to identify lncRNA genes that regulate NFkB signaling and monocyte to macrophage differentiation. NFkB signaling pathways have been extensively studied and protein-coding genes that regulate the signaling cascades have been considered mostly resolved (13, 37–39). Not only have we successfully identified lncRNA regulators of the TLR4/NFkB pathway, but we have also unveiled putative protein-coding regions pose a great challenge for functional characterization. By targeting these genes with CRISPRi, we may have simultaneously disrupted the function of the overlapping coding gene, regardless of how specifically targeted the dCas9-KRAB was to the lncRNA TSS. Despite this caveat, we have identified coding genes that function in this context. Further studies using classic CRISPR Cas9 to disrupt coding potential of these genes and measure effects on NFkB signaling are warranted to confirm that it is indeed the protein mediating the phenotype (*SI Appendix, Figs. S1 and S2*).

Although phenotypes associated with lncRNAs are often more subtle than those of proteins, we have used stringent analysis thresholds to bolster confidence in our list of functional lncRNA candidates. Notably, seven of our top hits were shared by the differentiation and inflammation screens implying dual roles for these genes. This overlap drew our attention to the lncRNA *LOUP* which shares a TAD with the myeloid fate-determining transcription factor SPI1. Both SPI1 and NFkB contribute to monocyte to macrophage differentiation, and both regulate inflammatory gene expression (40, 41). While the connections between SPI1 and NFkB signaling are not well elucidated, there is evidence that SPI1 plays a key role in both maintaining NFkB levels (29) and in altering the epigenetic landscape to modulate NFkB binding (42, 43).

Initially, we expected to find that the *LOUP* phenotype was the result of *cis* regulation of *SPI1* as evidenced by enhancer-conserved epigenetic marks at the *LOUP* locus (Fig. 2), as well as a recent report of enhancer RNA activity whereby *LOUP* RNA guides the transcription factor RUNX1 to the *SPI1* promoter (14). Surprisingly, despite near-complete CRISPRi knockdown (Figs. 3 and 4), loss of *LOUP* did not significantly impact *SPI1* transcription (Fig. 4), indicating that the enhancer function is maintained, perhaps due to low levels of *LOUP* escape from silencing. However, we also observed that *LOUP* RNA is primarily cytoplasmic and that knockdown did reduce SPI1 protein levels (Fig. 3), pointing to a *trans*-acting function for this gene, and supporting the results of our differentiation screen.

In further study of *LOUP*'s potential mechanism of action *in trans*, we analyzed Ribo-Seq data in THP1s and primary human macrophages. These data suggested potential translation of three sORFs from the *LOUP* transcript, belying its status as a noncoding RNA. We demonstrated that each of the sORFs could be translated when expressed with their native 5' UTRs. Interestingly, expression of the sORFs rescued *SPI1* protein levels in our *LOUP*-CRISPRi knockdowns, while expression of the *LOUP* RNA without start codons did not (Fig. 4). We also demonstrated that *LOUP* negatively regulates NFkB genes, perhaps through the translated sORFs, in agreement with our reporter screen result. Perplexingly *LOUP* KD causes both reduced SPI1 and upregulation of inflammatory genes including IL8, while *SPI1* KD with siRNA resulted in decreased IL8. We would generally expect SPI1 to positively regulate inflammatory genes in agreement with the siRNA result, so it may be that the sORFs are decreasing

inflammatory gene expression independent of their effect on SPI1, or that alternate feedback mechanisms are in play in the case of the longer duration CRISPRi experiments (relative to the fast siRNA experiments). In support of the former possibility, there are a growing number of cases highlighting synergistic or antagonistic functions of sORF encoded peptides (SEPs) and their host transcripts (16). For example, in the case of *MIR155HG* (another of our NFkB screen hits), the 17-amino acid peptide negatively regulates MHCII antigen presentation by directly binding HSC70 (22), while miRNA miR-155 broadly increases the inflammatory response including increasing MHCII presentation (44).

Here, we showcase the value of pooled CRISPRi screening as an efficient method to identify functional lncRNAs in the context of innate immunity. Meticulous control of macrophage signaling is crucial for a proper immune response, and the screens performed here have demonstrated that lncRNAs play an important role in maintaining these signaling pathways. Understanding lncRNA function in this context has led to insights into inflammatory gene regulation and even the bimodal functional capabilities of lncRNAs to regulate gene expression *in cis* and *trans*. Here, we described a role for a myeloid-specific lncRNA as a potent regulator of inflammatory gene expression. This work will serve as a valuable resource of both lncRNAs and coding genes involved in this pathway, as well as an important foundation for further mechanistic understanding of functional SEPs.

## Methods

**Cell Lines.** Wild-type (WT) THP1 cells were obtained from ATCC. All THP1 cell lines were cultured in RPMI 1640 supplemented with 10% low-endotoxin fetal bovine serum (ThermoFisher), 1X penicillin/streptomycin, and incubated at 37 °C in 5% CO<sub>2</sub>.

Mouse bone marrow-derived macrophages (BMDMs) were isolated from wild-type mice and immortalized using a CreJ2 virus as described previously (45). All mouse cell lines were cultured in DMEM supplemented with 10% low-endotoxin fetal bovine serum (ThermoFisher) and 1X penicillin/streptomycin. Cells were incubated at 37 °C in 5% CO<sub>2</sub>.

**Lentivirus production.** All constructs (*Dataset S9*) were cotransfected into HEK293T cells with lentiviral packaging vectors psPAX (Addgene cat#12260) and pMD2.g (Addgene cat#12259) using Lipofectamine 3000 (ThermoFisher cat# L3000001) according to the manufacturer's protocol. Viral supernatant was harvested 72 h posttransfection.

**THP1-NFkB-EGFP-dCasKRAB.** We constructed a GFP-based NFkB reporter system by adding 5 × NFkB-binding motifs (GGGAATTC) upstream of the minimal CMV promoter-driven EGFP. THP1s were lentivirally infected and clonally selected for optimal reporter activity. Reporter cells were then lentivirally infected with the dCas9 construct that was constructed using Lenti-dCas9-KRAB-blast, addgene#89567. Cells were clonally selected for knockdown efficiency greater than 90%.

**THP1-NFkB-EGFP-dCasKRAB-sgRNA (*LOUP* knockdown).** NFkB-EGFP-CRISPRi-THP1 cells were lentivirally infected with sgRNAs. sgRNA constructs were made from a pSico lentiviral backbone driven by an EF1a promoter expressing T2A flanked genes: puromycin resistance and mCherry. sgRNAs were expressed from a mouse U6 promoter. Twenty-nucleotide forward/reverse gRNA oligonucleotides were annealed and cloned via the AarI site.

**THP1-NFkB-EGFP-dCasKRAB-*LOUP*-/- sORF+.** sORF-GFP fragments were synthesized by Twist Biosciences and cloned into a pSico lentiviral backbone. Constructs were then packaged into lentiviral particles as described above and used to infect one of the CRISPRi *LOUP* knockdown lines (generated above). Unstimulated GFP+ cells were sorted by FACS on a BD FACS Aria II two times to achieve a 100% GFP-positive population assuming that GFP expression in unstimulated cells was not activation of the reporter. Cells were consistently cultured under blasticidin and puromycin to maintain active dCas9 and sgRNA expression.

**>sORF1-GFP.** atttattatagccATGAAATGCTCTGCTCTCTCTCTTTTCCTGCTGCCCTG GGGCTGGAGGAGCACGGGCTCCCCGGAGTGGGCTTCAGCTCCCGGTGGCCGGC GGAAGTGGAGGTGGAggctcagctGGTGAGGCAGTTCGgtgagcaaggcgagagctg

ttaccggggtgtgcccactctgtgagctgagcggcgacgtaaacggccacaagttagcgtgtccggc  
gagggcgagggcgatgccactacggcaagctgacccctgaagttcatctgacaccggcgaagctgcccgtg  
ccctggcccacctctgaccacccctgacctagcggctgagctgtcctgaccccgaccatgaagcag  
cagacttcttaagtcggcctgcccgaagctagctccaggagcgcacacttcttaaggagcggcaac  
tacaagaccggcggaggtgagttcggcggcagaccctgtgtaaccgcatcgatgtaagggcactc  
gactcaagggagcagcgaacatctggggcacaagctggaagtaactacaacagccacaacgtctatc  
atggcggcagaagcagaagcggcactcaagtgtaactcaagctcccaacaacatcgagcggcag-  
cgtgagctgcccaccactaccagagaacccccatcggcgacggcccgtgctgcccgaaccac-  
tactgagcaccagctccctgagcaagaccccaagcagaagcgcatcacatgtctctgagtg-  
tctgaccggcgggatcactctgcatgagcagctgtaacaagtag

**>SORF2-GFP.** atttattatagccatgaaATGCTCTGCTCTTCTCTTTCTGCTGT  
CCCTGGGGCTGGAGGAGCAGCCTCTCCCGGGAGTGGGCTTCAGCCTCC  
TAGACTCTGTCTCTTCCAGGGGCTAGCCTGGGGCAGGAGCAAGAGTCC  
CTAGAGCGTCCAAGATTTTGGTTTCAAACC AATTTCTCCGCGTGGCGCGGAA  
GTGAGAGTGAAGgctcagctGTGGAGGCAGTTCGgtgagcaagggcgaggagctgt  
tcaacggggtgtgcccactctgtgagctggaagcggcagcgtaaacggccacaagttagcgtg  
gttccgggagggcgagggcgatgccactacggcaagctgacctgaagttcatctgaccaccg  
gcaagctgcccgtccctggccaacctctgaccaccctgacctagcgtgagctgctcagcc  
gctaccccgaccatgaaagcagcagacttcttaagtcggcctgcccgaagcagctaccag  
agcgaccatcttcaagcagcggcaactacaagcccgccgagggtgaagttcagggcg  
acaacctgtgaaccgcatcgagctgaagggcactcgaagggagcggcaacatctctg  
ggcacaagctgagtagaactacaacagccaacagcttatactatgcccagacagcagaaga  
acgcatcaaggtgtaactcaagctcccaacacatcgaggagcggcagcgtgacgtcggcagc-  
cactaccagcagaacacccccatcggcgacggcccgtgctgcccgaacaacactcagag-  
caccagtcggccctgagcaagaccccaacgagaagcgcgcatcacatggtctctgagttcgt-  
gaccggcgggatcactctgcatgagcagctgtaacaagtag

**>SORF3-GFP.** ttgatcctgtctccctggggctggaggagcagggcctccccgggagtggtg  
cagcccttagactctgtctcccaagggtaggctgggggaccagaagcaagagctccatagagctcca  
agatTTTTgttcaaaccaattctctgtagcagaATGAATGGAGCCACATCCAGCAGATGCAC  
CTGCTGACTCTGCAAGTCAGGACCTCTCTGCCCTCTTTTGTCTGCTGTCAGGAGG  
GAGAAGCTGGAAATGTCTCTCTGTTGGTCCACTCCAGCAGCAGCAGTACTCCCTGT  
CTCCCCAAACCTCTCTGTTGCTCTCTCTGTCTCTCTCTCCATCTGCTCTGCGCCTG  
CTCTCTCTTTTCTGCTGAGGTTGCTGCTCTCTCTACCTCTTGTCTGTTCTCTCTCTC  
TGCTCCCTCTTgtggtcggcgaagtgagggtgaggtcagctggtggagcagttcgtgagcaag  
ggcgaggagctgttaccggggtgtgcccactctgtgagctgagcggcgacgtaaacggccaaagttc  
agcgtgctcggcagggcgagggcgatgccactacggcaagctgacctgaagttcatctgaccaccggc  
aagctgcccgtcccctgcccactctgtgaccacctgaacctagcggcgtgagctttagcggcaccggc  
cacatgaagcagcagcttctcaagtcggcctgcccgaaggtcagctcaggagcgcacatcttcaag  
gagcagggcaactacaagcccgccgaggtgaagttcagggcgacacctggtgaaccgcatcg  
ctgaagggcagctgactcaagggagcggcaacatctctgggcacaagctgagtagaactacaacagcca-  
acagctctatcatggtggcagaagcagaagcggcactcaaggtgtaactcaagctcccaacaacatcgag-  
gagcggcagctgagcggcaccactaccagcagaacccccatcggcgacggcccgtgctgcccga-  
caaccactactgagcaccagtcggcctgagcaagaccccaacgagaagcgcgcatcacatggtctgctg-  
gagttctgaccggcgggatcactctgcatgagcagctgtaacaagtag

**THP1-NFKB-EGFP-Cas9.** The NFKB reporter was introduced as described above. The Cas9 construct was constructed from a pSico lentiviral backbone with an EF1a promoter expressing T2A flanked genes: blasticidin-resistant (blast), blue fluorescent protein, and humanized *Streptococcus pyogenes* Cas9. Cells were clonally selected for knockdown efficiency greater than 90%.

**Primary Mouse Monocytes.** Primary mouse monocytes were isolated by performing bone marrow extraction from 6 C57BL/6 mice per replicate followed by monocyte isolation using the Monocyte Isolation Kit (Mouse) (Miltenyi, 130-100-629). Cells were cultured in DMEM supplemented with 10% heat-inactivated fetal bovine serum, 1X Pen Strep, and 1X Cipro. Cell lines cultured at 37 °C with 5% CO<sub>2</sub>.

**iBMDM-NFKB-EGFP-dCas9KRAB.** iBMDM-NFKB-EGFP reporter cells were then lentivirally infected with the dCas9 construct that was constructed using Lenti-dCas9-KRAB-blast, addgene#89567. Cells were clonally selected for knockdown efficiency greater than 90%. Cells were lentivirally infected with sgRNAs targeting *Loup* or nontargeting control. sgRNA constructs were generated as described above and are outlined in Dataset S9.

#### Screening Protocol.

**sgRNA library design and cloning.** Ten sgRNAs were designed for each TSS of hg19 annotated lncRNAs expressed in THP1s at baseline and upon stimulation. The sgRNA library also included 700 nontargeting control sgRNAs, and sgRNAs targeting 50 protein-coding genes as positive controls. The sgRNA library was designed and cloned as previously described in ref. 5.

**CRISPRi NFKB FACS screen.** Library infected and selected THP1-NFKB-EGFP-CRISPRi-sgRNA cells were expanded to 2,000× coverage. Cells were stimulated with LPS (200 ng/mL) for 24 h to induce expression of NFKB-EGFP. Flow cytometry and PCR amplification of genomic sgRNA sequences were conducted as previously described in detail in ref. 20. Screen was performed three times in THP1 lines (replicates A, B, C).

**NFKB screen analysis.** SgRNA guide adapters were removed with cutadapt (46), and counts were obtained with the MAGeCK count function from MAGeCK (47). Z-scores for each gene were found by analyzing each replicate independently with MAUDE (48). For each gene in the experiment, aggregate z-scores were generated using Stouffer's method, and a combined false-discovery rate was calculated. Data are available at GSE247761.

**CRISPRi PMA screen.** THP1-NFKB-EGFP-CRISPRi-sgRNA were infected with the sgRNA library as previously described for the NFKB screen. Cell lines were infected, and the initial coverage after infection was ~500 to 600×. Then, cells were expanded to >1,000× coverage. Triplicates were either left untreated or treated with 2 nM PMA on days 0, 8, and 9. Undifferentiated cells were collected on day 11, and sgRNAs were PCR amplified as previously described for the NFKB screen.

**PMA screen analysis.** SgRNAs were counted and passed to DESeq2 for analysis. Default normalization was performed, and log2foldchange (L2FC) was calculated for each sgRNA between the PMA and No Treatment conditions. L2FC for the set of sgRNAs targeting each gene were compared to L2FC of all negative controls by the Mann-Whitney U (MWU) test. PMA replicate B was excluded from the analysis as it fell below 500× sgRNA coverage over the course of the experiment. Data are available at GSE247761.

**Sequencing data.** Human RNA-Seq data are from ref. 49 and available at GSE147310. We previously published the mouse BMDM RNA-Seq Data (50), and they are available at GSE141754. Data pertaining to ATAC-Seq, ChIP-Seq, and HiC analyses in THP1s were originally reported in ref. 23 and are available at GEO: GSE96800 and SRA: PRJNA385337. Ribo-Seq data are from refs. 51–53, with data available at GSE208041, GSE66810, and GSE39561, respectively. BMDM CTCF ChIP-Seq is deposited at GSE36099 (54). BMDM ATAC-Seq and H3K27ac ChIP-Seq were used from the C57 strain deposited at GSE109965 (55). RNA-seq was performed on THP1-NFKB-EGFP-CRISPRi-sgRNA controls (nontargeting and anti-GFP) versus *LOUP* knockdown in monocytes (THP1s) and PMA-treated cells (macrophages). THP1 cells were stimulated with 100 nM PMA for 24 h. Data are available at GSE247761.

**ATAC and ChIP-Seq.** Adapters were trimmed with Ngsmerge (56) and mapped to GRCh38 primary assembly for humans, or GRCh38 for mice, with Bowtie2 (--very-sensitive --maxins 1000) (57). Replicates were merged, and alignments were converted to BigWig tracks with the bamCoverage (--binsize 1) module from deepTools (58).

**Liftover of mouse tracks.** Mouse alignments were lifted to GRCh38 with the "liftover" utility from the UCSC Genome Browser's kent tools using hg38.mm39.all.chain.gz. Alignments were visualized using pyGenomeTracks (59).

**HiC.** Paired-end reads from untreated or PMA-treated THP1s were deduplicated with BMap clumpify (dedupe=t ziplen=3 reorder=t compressmp=f deleteinput=t). Fastqs were converted to Pairs format with Chromap (-e 4 -q 1 --split-alignment --pairs) (60) and replicates were merged with Pairtools (61). Cool format files were generated with Cooler (cooler load pairs) at 5 kb resolution and then normalized with hicNormalize (-n smallest -sz 1.0) and Knight-Ruiz corrected with hicCorrectMatrix (--correctionMethod KR) (62). TADs were called with hicFindTADs (--minDepth 15000 --maxDepth 150000 --step 15000 --thresholdComparisons 0.05 --delta 0.01 --correctForMultipleTesting fdr) from the HiCExplorer suite (58).

**Differential transcript usage.** Mouse RNA-Seq was quantified with Salmon (63) against our previously published BMDM transcriptome (50). To reduce complexity, representative gene models were selected as in Dataset S8 to represent the isoforms of *Loup* and *Spi1*. TPMs were imported with Tximport (64) and relative transcript usage calculated with DRIMSeq (65) by treating the *Loup*, *Spi1\_AFE1*, and *Spi2\_AFE2*, all of which begin at the upstream exon, as a single feature.

**Ribo-Seq.** Adapters were removed with Cutadapt (46). A tRNA/rRNA index was built with Bowtie2 (56), and mapped reads were discarded. The remaining reads were mapped with STAR in end-to-end mode to the Hg38 genome, guided by a custom annotation set composed of Gencode v41 merged with the published isoform atlas from primary macrophages (25). Multimapping reads were discarded.

**Western Blotting.** Protein was isolated from cells by removing cell media, washing cells with 1 × PBS, and then lysing them with RIPA buffer plus protease inhibitor. Cell lysates were quantified by the Pierce™ BCA Protein Assay Kit. Equal amounts of protein (15 µg) of each sample were denatured at 70 °C for 10 min prior to loading on 10 or 12% SDS-PAGE. Samples were transferred to polyvinylidene difluoride (PVDF) membranes using the Trans-Blot Turbo Transfer System (Bio-Rad), blocked with TBST (1 × Tris-buffered saline with 0.1% Tween 20) supplemented with 5% (wt/vol) BSA for 1 h and blotted with PU.1 (9G7) (1:1000, Cell Signaling #2258) at 4 °C overnight. Horseradish peroxidase (HRP)-conjugated goat anti-rabbit (1:2,000, Bio-Rad, #1706515) secondary antibody was used. Western blots were developed using SuperSignal™ West Pico PLUS Chemiluminescent Substrate (Thermo Scientific cat# 34577). After imaging, HRP was inactivated for 2 h in 0.2% sodium azide in TBST supplemented with 5% (wt/vol) BSA. B-Actin (C4) monoclonal antibody (1:500, Santa Cruz Biotechnology cat #47778) was subsequently used as a loading control followed by HRP-conjugated goat anti-rabbit secondary antibody (1:2,000).

**siRNA Knockdown of SPI1.** WT THP1 cells or THP1-NFκB-EGFP were transfected with 60 pmol of SPI1 targeting (ThermoFisher cat# HSS186060) or Cy3-conjugated nontargeting siRNA (ThermoFisher cat# AM4621) for 72 h using Lipofectamine 3000 (ThermoFisher cat# L3000001) according to the manufacturer's protocol.

**Nanostring Multiplexed Transcript Analysis.** RNA was isolated using the Direct-zol RNA Miniprep Plus Kit (Zymo cat# R2052) from one control and two LOUP knockdown THP1 cell lines at baseline and after 6 h of LPS treatment. RNA was quantified on a Nanodrop. Of note, 100 ng of RNA was used for each sample hybridization (Nanostring Master Kit cat# 100052) and detection with the Nanostring Human Immunology V2 nCounter GX Codeset (cat# 115000062) on a MAX/Flex nCounter according to the manufacturer's protocol.

**ELISA and Multiplexed ELISA.** WT THP1 cells transfected with SPI1 targeting siRNAs were seeded at equal densities and stimulated with LPS for 24 h. Samples were diluted 1:10 and IL8 was measured using the DuoSet IL8 ELISA kit (R&D Systems cat# DY208) following the manufacturer's protocol. THP1-NFκB-EGFP-CRISPRi-sgRNA LOUP knockdown and control cells were seeded at equal densities and treated with LPS for 24 h. Then, 75 µL of supernatants were collected and analyzed undiluted by EVE Technologies using their Human Cytokine Panel A 48-Plex Discovery Assay (cat# HD48A).

**Nuc/Cyt Fractionation and RT-qPCR.** WT THP1 cells were fractionated according to the NE-PER kit protocol (ThermoFisher cat# 78833) with RNase inhibitor (Superase-IN, ThermoFisher cat# AM2696) added to the cytosolic and nuclear lysis buffers. Three volumes of Trizol (TRI Reagent, Sigma T9424) was added to the fractions and RNA was isolated using the Direct-zol RNA Miniprep Plus Kit (Zymo cat# R2052). Then, 16 µL of RNA isolated from fractions was reverse transcribed (iScript cDNA synthesis kit, Bio-Rad cat# 1708840) followed by qPCR (iTaQ SYBRgreen Supermix, Bio-Rad cat# 1725121) using the cycling conditions as follows: 50 °C for 2 min, 95 °C for 2 min followed by 40 cycles of 95 °C for 15 s, 60 °C for 30 s, and 72 °C for 45 s.

**RNA Isolation and RT-qPCR of Primary Mouse Monocytes.** RNA was extracted from primary mouse monocytes following treatment with 200 ng/mL LPS for 2 or 6 h or no treatment. RNA was isolated by phenol chloroform extraction and ethanol precipitation as follows: RNA sample mixed in a 5:1 ratio of tri-reagent

(Sigma Aldrich, T9424-200 mL) to chloroform (Ricca, RSOC0020-500C) and sample spun at the maximum speed for 20 min at 4 °C in gel-heavy tubes. The upper aqueous layer was removed to a new tube and mixed 1:1 with isopropanol (Fisher Scientific, BP2618-4) and incubated for 1 min with glycoblue coprecipitant (Invitrogen, AM9515). The sample was spun for 5 min at the maximum speed at 4 °C. The supernatant was discarded, and the pellet was washed with cold 75% ethanol and spun at the maximum speed at 4 °C for 2 min 2 ×, discarding supernatant between spins. The pellet was air dried for 1 min. The sample was subjected to DNaseI treatment (New England Biolabs, M0303S) at 37 °C for 30 min. After DNase treatment, 2 × NT2 buffer and equal total volume of lower layer of phenol/chloroform/isoamyl alcohol (Fisher Scientific, BP17521-400) were added, vortexed, and spun at room temperature for 5 min at a maximum speed. The upper aqueous layer was transferred to a new tube and mixed with sodium acetate to a final concentration of 0.3 M, 2.5 × 100% EtOH, and glycoblue coprecipitant prior to precipitation at –80 °C for 1 to 3 d. The sample was spun at the maximum speed for 30 min, and the supernatant discarded. The pellet was washed with 75% EtOH and spun 2 min at 4 °C 2 ×, discarding the supernatant in between. The pellet was air dried RT 2 min and resuspended in DEPC water.

RNA was quantified using the Qubit RNA HS kit (Invitrogen, Q32852). Equal amounts of RNA per replicate (250 to 560 ng) were reverse transcribed into cDNA using iScript Reverse Transcription Supermix reagent (BioRad, 1708890). cDNA was diluted 1:30, and qPCR was performed using primers against murine HPRT and murine LOUP and iTaQ Universal Sybr Green Supermix (BioRad, L001751B) with the following cycling conditions: 95 °C for 10 min, followed by 41 cycles of 95 °C for 15 s, 60 °C for 30 s, 72 °C for 30 s, followed by 95 °C for 10 s and a melt curve from 55 to 95 °C at 0.5 °C per second. Primer sequences for mice can be found in [Dataset S9](#). Gene expression was normalized to HPRT.

**RNA Isolation and RT-qPCR.** Cells were homogenized in Tri-Reagent (Sigma Aldrich, T9424-200 mL). RNA was extracted with the Direct-zol RNA miniprep plus RNA extraction Kit (Zymo, R2072). One µg of total RNA was reverse transcribed into cDNA (iScript cDNA synthesis kit, Bio-Rad cat# 1708840). cDNA was diluted 1:30 in qPCR experiments. Cycling conditions are the same as above for primary mouse monocytes.

**Data, Materials, and Software Availability.** All data has been deposited as described in the materials and methods under [GSE247761](#) (66). All other study data are included in the article and/or [supporting information](#).

**ACKNOWLEDGMENTS.** S. Carpenter is supported by R35GM137801 from NIGMS, and E.M. is supported by F31AI179201 from NIAID.

Author affiliations: <sup>a</sup>Department of Molecular, Cell and Developmental Biology, University of California Santa Cruz, CA 95064; <sup>b</sup>Department of Biomolecular Engineering, University of California Santa Cruz, CA 95064; <sup>c</sup>Department of Radiation Oncology, University of California, San Francisco, CA 94158; <sup>d</sup>Department of Neurological Surgery, University of California, San Francisco, CA 94158; <sup>e</sup>Department of Pediatrics, Division of Genetics and Genomics, Boston Children's Hospital, Boston, MA 02115; <sup>f</sup>Department of Stem Cell and Regenerative Biology, Harvard University, Cambridge, MA 02138; <sup>g</sup>Whitehead Institute for Biomedical Research, Massachusetts Institute of Technology, Cambridge, MA 02142; <sup>h</sup>HHMI, Chevy Chase, MD 20815; <sup>i</sup>David H. Koch Institute for Integrative Cancer Research, Massachusetts Institute of Technology, Cambridge, MA 02142; and <sup>j</sup>Department of Biology, Massachusetts Institute of Technology, Cambridge, MA 02142

Author contributions: H.H., S. Covarrubias, J.S.W., and S. Carpenter designed research; H.H., E.M., S. Covarrubias, S.Y., C.M., L.S., L.N., and S. Carpenter performed research; S.J.L., M.A.H., and J.S.W. contributed new reagents/analytic tools; H.H., E.M., S. Covarrubias, S.K., and S. Carpenter analyzed data; and H.H., E.M., S. Covarrubias, and S. Carpenter wrote the paper.

1. M. N. Cabili *et al.*, Integrative annotation of human large intergenic noncoding RNAs reveals global properties and specific subclasses. *Genes Dev.* **25**, 1915–1927 (2011).
2. A. Bhan, M. Soleimani, S. S. Mandal, Long noncoding RNA and cancer: A new paradigm. *Cancer Res.* **77**, 3965–3981 (2017).
3. M. Guttman *et al.*, lincRNAs act in the circuitry controlling pluripotency and differentiation. *Nature* **477**, 295–300 (2011).
4. E. K. Robinson, S. Covarrubias, S. Carpenter, The how and why of lincRNA function: An innate immune perspective. *Biochim. Biophys. Acta Gene Regul. Mech.* **1863**, 194419 (2020).
5. S. J. Liu *et al.*, CRISPRi-based genome-scale identification of functional long noncoding RNA loci in human cells. *Science* **355**, aah7111 (2017).
6. Y. Liu *et al.*, Genome-wide screening for functional long noncoding RNAs in human cells by Cas9 targeting of splice sites. *Nat. Biotechnol.* **36**, 1203–1210 (2018).
7. J. R. Haswell *et al.*, Genome-wide CRISPR interference screen identifies long non-coding RNA loci required for differentiation and pluripotency. *PLoS One* **16**, e0252848 (2021).
8. S. Zhu *et al.*, Genome-scale deletion screening of human long non-coding RNAs using a paired-guide RNA CRISPR-Cas9 library. *Nat. Biotechnol.* **34**, 1279–1286 (2016).
9. C. Arnan *et al.*, Paired guide RNA CRISPR-Cas9 screening for protein-coding genes and lncRNAs involved in transdifferentiation of human B-cells to macrophages. *BMC Genomics* **23**, 402 (2022).
10. C. Auffray, M. H. Sieweke, F. Geissmann, Blood monocytes: Development, heterogeneity, and relationship with dendritic cells. *Annu. Rev. Immunol.* **27**, 669–692 (2009).
11. A. Sica, A. Mantovani, Macrophage plasticity and polarization: In vivo veritas. *J. Clin. Invest.* **122**, 787–795 (2012).
12. S. L. Orozco, S. P. Canny, J. A. Hamerman, Signals governing monocyte differentiation during inflammation. *Curr. Opin. Immunol.* **73**, 16–24 (2021).
13. M. R. Zinatizadeh *et al.*, The Nuclear Factor Kappa B (NF-κB) signaling in cancer development and immune diseases. *Genes Dis.* **8**, 287–297 (2021).
14. B. Q. Trinh *et al.*, Myeloid lncRNA LOUP mediates opposing regulatory effects of RUNX1 and RUNX1-ETO in t(8;21) AML. *Blood* **138**, 1331–1344 (2021).



15. N. Hah *et al.*, Inflammation-sensitive super enhancers form domains of coordinately regulated enhancer RNAs. *Proc. Natl. Acad. Sci. U.S.A.* **112**, E297–E302 (2015).
16. E. Malekos, S. Carpenter, Short open reading frame genes in innate immunity: From discovery to characterization. *Trends Immunol.* **43**, 741–756 (2022).
17. M. Kampmann, M. C. Bassik, J. S. Weissman, Integrated platform for genome-wide screening and construction of high-density genetic interaction maps in mammalian cells. *Proc. Natl. Acad. Sci. U.S.A.* **110**, E2317–E2326 (2013).
18. S. Covarrubias *et al.*, CRISPR/Cas-based screening of long non-coding RNAs (lncRNAs) in macrophages with an NF- $\kappa$ B reporter. *J. Biol. Chem.* **292**, 20911–20920 (2017).
19. R. She, J. Luo, J. S. Weissman, Translational fidelity screens in mammalian cells reveal eIF3 and eIF4G2 as regulators of start codon selectivity. *Nucleic Acids Res.* **51**, 6355–6369 (2023).
20. S. Covarrubias *et al.*, High-throughput CRISPR screening identifies genes involved in macrophage viability and inflammatory pathways. *Cell Rep.* **33**, 108541 (2020).
21. J. Rosenbluh *et al.*, Complementary information derived from CRISPR Cas9 mediated gene deletion and suppression. *Nat. Commun.* **8**, 15403 (2017).
22. L. Niu *et al.*, A micropeptide encoded by lncRNA MIR155HG suppresses autoimmune inflammation via modulating antigen presentation. *Sci. Adv.* **6**, eaaz2059 (2020).
23. D. H. Phanstiel *et al.*, Static and dynamic DNA loops form AP-1-bound activation hubs during macrophage development. *Mol. Cell* **67**, 1037–1048.e6 (2017).
24. D. Hnisz *et al.*, Super-enhancers in the control of cell identity and disease. *Cell* **155**, 934–947 (2013).
25. A. C. Vollmers, H. E. Mekonen, S. Campos, S. Carpenter, C. Vollmers, Generation of an isoform-level transcriptome atlas of macrophage activation. *J. Biol. Chem.* **296**, 100784 (2021).
26. S. Carpenter *et al.*, A long noncoding RNA mediates both activation and repression of immune response genes. *Science* **341**, 789–792 (2013).
27. A. F. Groff *et al.*, In vivo characterization of Linc-p21 reveals functional cis-regulatory DNA elements. *Cell Rep.* **16**, 2178–2186 (2016).
28. S. Ghisletti *et al.*, Identification and characterization of enhancers controlling the inflammatory gene expression program in macrophages. *Immunity* **32**, 317–328 (2010).
29. M. Karpurapu *et al.*, Functional PU.1 in macrophages has a pivotal role in NF- $\kappa$ B activation and neutrophilic lung inflammation during endotoxemia. *Blood* **118**, 5255–5266 (2011).
30. S. A. Turkistany, R. P. DeKoter, The transcription factor PU.1 is a critical regulator of cellular communication in the immune system. *Arch. Immunol. Ther. Exp. (Warsz)* **59**, 431–440 (2011).
31. G. Natoli, S. Ghisletti, I. Barozzi, The genomic landscapes of inflammation. *Genes Dev.* **25**, 101–106 (2011).
32. T. Fukui *et al.*, Involvement of PU.1 in the transcriptional regulation of TNF- $\alpha$ . *Biochem. Biophys. Res. Commun.* **388**, 102–106 (2009).
33. N. Ueno *et al.*, PU.1 acts as tumor suppressor for myeloma cells through direct transcriptional repression of IRF4. *Oncogene* **36**, 4481–4497 (2017).
34. J. Ruiz-Orera, X. Messeguer, J. A. Subirana, M. M. Albà, Long non-coding RNAs as a source of new peptides. *eLife* **3**, e03523 (2014).
35. Y. Gu, Y. Mao, L. Jia, L. Dong, S.-B. Qian, Bi-directional ribosome scanning controls the stringency of start codon selection. *Nat. Commun.* **12**, 6604 (2021).
36. J. Jumper *et al.*, Highly accurate protein structure prediction with AlphaFold. *Nature* **596**, 583–589 (2021).
37. T. D. Gilmore, The Rel/NF- $\kappa$ B signal transduction pathway: Introduction. *Oncogene* **18**, 6842–6844 (1999).
38. M. Neumann, M. Naumann, Beyond IkappaBs: Alternative regulation of NF- $\kappa$ B activity. *FASEB J.* **21**, 2642–2654 (2007).
39. A. Verma *et al.*, Transcriptome sequencing reveals thousands of novel long non-coding RNAs in B cell lymphoma. *Genome Med.* **7**, 110 (2015).
40. V. Bottero, S. Withoff, I. M. Verma, NF- $\kappa$ B and the regulation of hematopoiesis. *Cell Death Differ.* **13**, 785–797 (2006).
41. J. Minderjahn *et al.*, Mechanisms governing the pioneering and redistribution capabilities of the non-classical pioneer PU.1. *Nat. Commun.* **11**, 402 (2020).
42. S.-D. Ha, W. Cho, R. P. DeKoter, S. O. Kim, The transcription factor PU.1 mediates enhancer-promoter looping that is required for IL-1 $\beta$  eRNA and mRNA transcription in mouse melanoma and macrophage cell lines. *J. Biol. Chem.* **294**, 17487–17500 (2019).
43. F. Jin, Y. Li, B. Ren, R. Natarajan, PU.1 and C/EBP(alpha) synergistically program distinct response to NF- $\kappa$ B activation through establishing monocyte specific enhancers. *Proc. Natl. Acad. Sci. U.S.A.* **108**, 5290–5295 (2011).
44. J. Hodge *et al.*, Overexpression of microRNA-155 enhances the efficacy of dendritic cell vaccine against breast cancer. *Oncoimmunology* **9**, 1724761 (2020).
45. D. De Nardo, D. V. Kalvakolanu, E. Latz, Immortalization of murine bone marrow-derived macrophages. *Methods Mol. Biol.* **1784**, 35–49 (2018).
46. M. Martin, Cutadapt removes adapter sequences from high-throughput sequencing reads. *EMBnet.J.* **17**, 10–12 (2011).
47. W. Li *et al.*, MAGeCK enables robust identification of essential genes from genome-scale CRISPR/Cas9 knockout screens. *Genome Biol.* **15**, 554 (2014).
48. C. G. de Boer, J. P. Ray, N. Hacohen, A. Regev, MAUDE: Inferring expression changes in sorting-based CRISPR screens. *Genome Biol.* **21**, 134 (2020).
49. R. Song *et al.*, IRF1 governs the differential interferon-stimulated gene responses in human monocytes and macrophages by regulating chromatin accessibility. *Cell Rep.* **34**, 108891 (2021).
50. E. K. Robinson *et al.*, Inflammation drives alternative first exon usage to regulate immune genes including a novel iron-regulated isoform of Aim2. *Elife* **10**, e69431 (2021).
51. S. A. Ansari *et al.*, Integrative analysis of macrophage ribo-Seq and RNA-Seq data define glucocorticoid receptor regulated inflammatory response genes into distinct regulatory classes. *Comput. Struct. Biotechnol. J.* **20**, 5622–5638 (2022).
52. C. Fritsch *et al.*, Genome-wide search for novel human uORFs and N-terminal protein extensions using ribosomal footprinting. *Genome Res.* **22**, 2208–2218 (2012).
53. X. Su *et al.*, Interferon- $\gamma$  regulates cellular metabolism and mRNA translation to potentiate macrophage activation. *Nat. Immunol.* **16**, 838–849 (2015).
54. M. Garber *et al.*, A high-throughput chromatin immunoprecipitation approach reveals principles of dynamic gene regulation in mammals. *Mol. Cell* **47**, 810–822 (2012).
55. V. M. Link *et al.*, Analysis of genetically diverse macrophages reveals local and domain-wide mechanisms that control transcription factor binding and function. *Cell* **173**, 1796–1809.e17 (2018).
56. J. M. Gaspar, NGmerge: Merging paired-end reads via novel empirically-derived models of sequencing errors. *BMC Bioinformatics* **19**, 536 (2018).
57. B. Langmead, S. L. Salzberg, Fast gapped-read alignment with Bowtie 2. *Nat. Methods* **9**, 357–359 (2012).
58. F. Ramírez *et al.*, deepTools2: A next generation web server for deep-sequencing data analysis. *Nucleic Acids Res.* **44**, W160–W165 (2016).
59. L. Lopez-Delisle *et al.*, pyGenomeTracks: Reproducible plots for multivariate genomic datasets. *Bioinformatics* **37**, 422–423 (2021).
60. H. Zhang *et al.*, Fast alignment and preprocessing of chromatin profiles with Chromap. *Nat. Commun.* **12**, 6566 (2021).
61. Open2C, *et al.*, Pairtools: From sequencing data to chromosome contacts. bioRxiv [Preprint] (2023). <https://doi.org/10.1101/2023.02.13.528389> (Accessed 15 February 2023).
62. N. Abdennur *et al.*, Cooler: scalable storage for Hi-C data and other genomically labeled arrays. *Bioinformatics* **36**, 311–316 (2020).
63. R. Patro, G. Duggal, M. I. Love, R. A. Irizarry, C. Kingsford, Salmon provides fast and bias-aware quantification of transcript expression. *Nat. Methods* **14**, 417–419 (2017).
64. C. Sonesson, M. I. Love, M. D. Robinson, Differential analyses for RNA-seq: Transcript-level estimates improve gene-level inferences. *F1000Res* **4**, 1521 (2015).
65. M. Nowicka, M. D. Robinson, DRIMSeq: A Dirichlet-multinomial framework for multivariate count outcomes in genomics. *F1000Res* **5**, 1356 (2016).
66. H. Halasz, E. Malekos, S. Covarrubias, S. Carpenter, High throughput screens identify long non-coding RNA LOUP contributions to NFkB signaling and monocyte differentiation. GEO. <https://www.ncbi.nlm.nih.gov/geo/query/acc.cgi?acc=GSE247761>. Deposited 14 November 2023.